

Estimating and Identifying Parameters from Charge-Discharge Curves of Lithium-ion Batteries

Yanbo Qi^a, Suryanarayana Kolluri^a, Daniel T. Schwartz^a, Venkat R. Subramanian^{a,b}

^a Department of Chemical Engineering, University of Washington, Seattle, WA
98125, USA

^b Pacific Northwest National Laboratory, Richland, WA 99352 USA

Abstract

Electrochemical models for the lithium-ion battery are useful in predicting and controlling its performance. The values of the parameters in these models are vital to their accuracy. However, not all parameters can be measured precisely, especially when destructive methods are prohibited. In this paper, we proposed a parameter estimation approach to estimate the open circuit potential of the positive electrode (U_p) using piecewise linear approximation together with all the other parameters of a single particle model. Using the genetic algorithm (GA), U_p and 10 more parameters were estimated from a single discharge curve without knowledge of the electrode chemistry. Different case studies were presented for estimating U_p with different types of parameters of the battery model. The estimated parameters were then validated by comparing simulations at different C rates with experimental data.

Introduction

Due to their high power and energy densities, lithium-ion batteries are emerging as one of the most popular energy storage technologies, both for consumer electronics like mobile phones, and for now ubiquitous electric vehicles and grid scale energy storage. All lithium-ion battery installations are accompanied with a control system called the Battery Management System (BMS). The role of a BMS is to ensure safe and reliable operation of the battery and to perform functions like current, voltage and temperature monitoring. Based on these monitored inputs together with a battery model, a BMS generates operating decisions for the battery, including depth of discharge, charging profile and so on. Compared with conventional empirical models used in the BMS, sophisticated physics-based models can describe the battery dynamics more accurately, thus are able to suggest optimal charging profiles that reduce degradation while allowing greater depth of discharge. However, the lack of accurate parameters needed for these models, typically the Single Particle Model (SPM) or the Pseudo 2-Dimensional (P2D) Model, prevents their industry-wide adoption and general usage.

The parameters are generally not known, as battery manufacturers treat them as trade secrets. Some parameters like the electrode thickness and particle size are not difficult to measure after opening up the cell, while some parameters are almost impossible to measure experimentally even with time-consuming destructive methods. For example, Bruggeman coefficient and tortuosity cannot be measured directly, therefore usually require fitting the simulation results from the experimental data. The kinetic data on the insertion reactions are not available, because of the fast charge transfer and slow mass transfer in the system, thus is usually estimated. Furthermore, some parameters are function of battery configuration and usage, hence may vary from cell to cell and change during the battery's lifetime. The fact that battery parameters change with use,

makes direct measuring almost impossible, when updating the ‘instantaneous’ battery parameters over time is required for more accurate battery monitoring and control. The ability to get real-time parameters without opening up the cell is also important as greater proliferation of Lithium-ion batteries creates huge secondary usage market, which can only aim to use the batteries effectively and safely if the ‘instantaneous’ battery parameters are known.

Many efforts have been made for parameter estimation in the past. Commonly used methods include Electrochemical Impedance Spectroscopy (EIS), equivalent circuit model-based prediction with various Kalman filter methods, least squares method, machine learning etc. A detailed review of aforementioned methods can be found in Fleischer et al.¹.

Realizing the importance of parameter estimation in electrochemical models, many researchers have been actively working on this topic. Santhanagopalan and coworkers² applied the Levenberg-Marquardt method, a nonlinear least squares regression technique to both SPM and P2D models, and estimated diffusivity in positive electrode, reaction rate constants and initial SOCs in both electrodes from both charge and discharge curve. Ramadesigan et al.³ included capacity fade mechanism in their reformulated P2D model, and estimated the values of diffusivities in positive electrode and electrolyte and reaction rate constants in both electrodes over cycles using least squares estimation with Markov Chain Monte Carlo method for uncertainty quantification. Joel C. Forman and coworkers⁴ used genetic algorithm (GA) for P2D model together with Fisher identification and successfully optimized 88 parameters at the same time for the lithium iron phosphate cell. Using a modified GA method NSGAI with TOPSIS, Zhang et al.⁵ performed multi-objective parameter identification on both lithium-cobalt-oxide and lithium-iron-phosphate cells with thermal effects. More recently, Jun Li and coworkers used a heuristic algorithm to reduce the computational time during GA to estimate all parameters of a P2D model⁶.

However, in literature no one has reported successful estimation of thermodynamics parameters, the OCP of a single electrode (U_p). In this work, we proposed the estimation of U_p , as well as other parameters for a single particle model. U_p was approximated as a piecewise linear model without any knowledge of the electrode chemistry. The values of the piecewise linear U_p points were treated as additional parameters of the single particle model and were estimated to match a constant rate (1C) discharge curve obtained experimentally. Different case studies are presented to estimate U_p along with different types of parameters of the battery model.

Relevance

In this work, we proposed a methodology and initial results for estimating battery parameters, including the thermodynamic parameters of a single electrode based on just discharge curves. With further attempts to reduce the computational time, the proposed methodology can be deployed on-site in field systems to estimate the battery parameters on the fly. This opens up the door for system integrators to pick any cell on the market and use it in the most efficient way, with just the information provided in the battery datasheet. Since this method has the potential of real-time parameter estimation during operation, the parameters can be updated every few cycles to reflect the change in the cell. It can also facilitate the usage of second-hand batteries, even when operating history was unavailable.

Single Particle Model

Electrochemical models for batteries usually fall into two categories, single particle model or P2D model. P2D model, also known as the Doyle-Fuller-Newman (DFN) model or porous electrode model, was developed by the Newman group in the 1990s⁷, which takes into account the porous electrode theory, concentrated electrolyte theory, Ohm's law, charge and material balance, and reaction kinetics. SP model was introduced into lithium-ion battery modeling later by the White group⁸ in the 2000s. The SP model is simpler compared to the P2D model but still captures the main physical processes in battery cells, including diffusion in the solid phase, reaction kinetics at the solid-electrolyte interphase, and material and charge balance. A more thorough comparison of battery models can be found in Ramadesigan et al⁹.

We used the SP model in this work, because it is less computationally expensive while still gives good results compared to experimental data in lower rates. SP model uses two particles with the averaged properties to represent the positive and negative electrode. The equations are listed in Table 1. For the negative electrode, we assumed it is graphite, and used a regression model to represent the Un-SOC relationship.

For cell voltage, we included a lumped parameter R_c , mainly for contact resistance at the current collector/electrode interface and the initial solid-electrolyte interface (SEI) layer resistance. The value for R_c is left as an adjustable parameter to be estimated at the beginning, and kept the same for other cases for simplicity, since it does not change much in a couple cycles. For the battery life simulation, the resistance may be a good representation of degradation over time.

Besides U_p , U_n , there are 10 other parameters in the SP model, namely diffusivity of positive and negative electrodes (D_p^s, D_n^s), reaction rate constants (k_p, k_n), electrode thicknesses (l_p, l_n), electrode porosities (ϵ_p, ϵ_n), and particle sizes (R_p, R_n). We then grouped the parameters into three groups, transport parameters (D_p^s, D_n^s), kinetic parameters (k_p, k_n), and design parameters ($l_p, l_n, \epsilon_p, \epsilon_n, R_p, R_n$). The design parameters can be measure more easily compared to the transport and kinetic parameters when destructive experiments are allowed. Therefore, we prioritize the estimation of the 10 parameters. We explored the estimation of U_p with transport parameters first, then included kinetic parameters, and eventually added design parameters.

To solve the SP model efficiently, finite difference method was applied for spatial discretization. For finite difference method, the more node points used, the more accurate the solution is, but the more computational cost required. We did simulations with 5, 10, 15, and 20 node points, shown in Figure 2. From the figure, the curve with 5 node points is slightly different from the rest near 3400s, suggesting that at least 10 points are needed for accurate simulation. We used 15 node points for rest of the work to ensure precise numerical solution for the model.

Estimation of U_p and Other Parameters

Similar to the work done by Ramadesigan et al.⁵, we used the least squares estimation approach to minimize the sum of squared differences between the experimental data and the model predictions. The objective function we used was

$$\min \sum_{t_0=0}^{t_n=lf} [V_{\text{exp}}(t_i) - V_{\text{model}}(t_i)]^2 \quad (1)$$

The experimental data was collected by discharging a fully charged Panasonic NCR18650A cell to 2.5 V at constant rates. The experimental data was recorded every second, resulting in ~3600 data points for 1C discharge. To reduce the number of data points, we used 1 point for every 10s, thus for 1C discharge, the number of data points was ~360. The typical nominal capacity of the cell is 3070mAh. The chemistry of the cell is not disclosed in its datasheet other than that it uses a nickel oxide system. It is common for commercial batteries to not disclose their chemistry, especially for positive electrode, making our work for estimation of U_p relevant.

Due to the complexity and nonlinearity of the electrochemical model, and the large number of parameters involved (in this work, 21 U_p s and other parameters), parameter optimization can be very challenging and computationally expensive. Genetic algorithm (GA) has been a popular approach recently for parameter estimation of electrochemical models⁶. GA is a global optimizer based on the process of natural selection and biological evolution. At every step (generation), a certain number (population) of individual solutions are randomly selected by mutation, crossover and selection from the previous generation. In this work, we used the Global Optimization Toolbox in MATLAB for GA.

Open Circuit Potential of the Positive Electrode

Owing to the existence of multi-stage intercalation voltage plateaus, the OCP-SOC relationship of a single electrode cannot be predicted by the general Nernst equation. The conventional way of getting the OCP information of a single electrode is by fitting a regression model to the experimental data measured at different state of charge (SOC)¹⁰. The OCP data is usually obtained by super slow discharge (at least 1/10C, sometimes as low as 1/60 C and even 1/100C) while measuring the potential vs. lithium metal as SOC changes. OCP is an intrinsic property of a certain material, thus needs to be determined every time when new electrode chemistry is used (eg. NCM¹¹, LCO¹²). The measurement is not only time consuming, but also destructive, as measurements need to be done for positive and negative electrode separately. Sometimes the experimental measurement can be spared if the chemistry of both electrodes is known and has been characterized, though the OCP-SOC relationship is not exactly the same for each individual cell even for the same materials fabricated with the same structures¹³. This relationship also changes as battery ages, resulting in bigger discrepancy in battery simulation. Furthermore, there are times when detailed material information is inaccessible, especially for commercial cells. As an alternative way to obtain single electrode OCP, estimation based on model-experimental comparison can be useful in practice.

In this study, we proposed a methodology to estimate U_p based on a single discharge curve. It can be used during the first several cycles, to calibrate the initial status of an individual cell. This method can also be used anytime during the lifetime of a battery to help track and account for the degradation over cycles.

The most common electrode OCP-SOC relationship is of certain polynomial form. As a first attempt, we used a third-order polynomial fit for the Up-SOC relationship, shown in Equation 1.

$$U_p = a\theta^3 + b\theta^2 + c\theta + d \quad (2)$$

Where a, b, c, and d are parameters to be estimated. We assumed that all the other parameters needed for the model are known, and used some guess values (listed as base case in Table 2.2) to estimate a, b, c, and d only. The best fit was plotted in Figure 3, together with the corresponding experimental data. As can be seen from the figure, the fit is far from reasonable. One can argue that by increasing the order of the polynomial function, the fit will be better and better. However, increasing the order of the Up-SOC function will dramatically increase the computational difficulty of the optimization problem. As a result, it is not favorable to pursue the polynomial fit function.

A piecewise linear approximated model for Up was used in this study. We picked a certain number of Up values at equally spaced SOCs, and used a linear relationship for the SOCs between two values we picked, as expressed in Equation 2.

$$U_{p,i+1} = U_{p,i} + (U_{p,i+1} - U_{p,i}) \times \frac{\theta_p^s - \theta_{p,i}^s}{\theta_{p,i+1}^s - \theta_{p,i}^s}, \forall i = 1 \dots \infty \quad (3)$$

In this work, we mainly focused on estimating the Up. We chose positive electrode because the lithium-ion batteries commercially available now mainly use graphite based negative electrode, but the positive electrode material varies from a group of lithium metal oxides and the combination of them. The exact material formula and properties of positive electrode are generally not known, causing extra difficulty in battery management.

Case Studies

In this section, the results from several case studies estimating Up and other parameters in the model will be presented to demonstrate our idea. All the case studies were performed based on a single discharge curve at 3000mA at room temperature, roughly 1C. For the parameters not estimated in a certain case, we are using $\pm 1\%$ of the respective values in the 7th column of Table 2.2 as bounds, and estimating at the same time, thus the total numbers of parameter to be estimated are the same (31) for all cases.

Case Study 1: Estimation of Up and Resistance

Our first attempt was to try out the idea of using linear model to approximate Up. We estimated Up for different n linear approximated variables, where $n = 4, 7, 13,$ and 21 Up values (Figure 4). Theoretically, when n is getting closer to infinity, the linear model is the same as the real case, but with a bigger n , the computational cost increases. We selected $n = 21$ for all the studies in this paper, because 21 points can give us a smooth and accurate enough discharge curve without an unaffordable computational expense. In this case, 21 points of the Up and the contact resistance were estimated using GA for SP model. The upper and lower bounds for the Up values were 2.5 V to 4.4 V. We added another constraint for the Up values such that they decrease as the SOC of the positive electrode increases, demonstrated in Equation 4.

$$U_{p,i+1} - U_{p,i} \leq 0, \forall i = 1 \dots \infty \quad (4)$$

The upper and lower bounds for K_R were 0.2Ω and 0.01Ω . No additional information about the electrode chemistry was required for the optimization. The estimated Up values were listed in the second column of Table 2.1 and plotted in Figure 5, while the discharge curve with estimated values can be found in Figure 6. As can be seen from Figure 6, the estimated curve matches well with the experimental data, suggesting that our linear approximation approach is applicable to the Up.

Case Study 2: Estimation of Up and Transport Parameters

With the success of Case 1, the next step would be to increase the number of parameters actually estimated. The transport and kinetic parameters are harder to measure, thus we estimated them together with the Up first. For Case 2, we set the resistance to be 0.0615Ω from Case 1, and estimated 21 Up values with transport parameters. The bounds for D_p^s and D_n^s were given as $3.34e-13 \text{ m}^2 \text{ s}^{-1}$ to $1e-12 \text{ m}^2 \text{ s}^{-1}$ and $1e-12 \text{ m}^2 \text{ s}^{-1}$ to $3e-12 \text{ m}^2 \text{ s}^{-1}$. The results are shown in Figures 5, 7, and Tables 2.1 and 2.2.

Case Study 3: Estimation of Up, Transport and Kinetic Parameters

We included the kinetic parameters together with Up values and transport parameters in this case. The bounds for D_p^s and D_n^s were given as $3.34e-13 \text{ m}^2 \text{ s}^{-1}$ to $1e-12 \text{ m}^2 \text{ s}^{-1}$ and $1e-12 \text{ m}^2 \text{ s}^{-1}$ to $3e-12 \text{ m}^2 \text{ s}^{-1}$. The bounds for k_p and k_n were $6.67e-12 \text{ m}^{2.5} \text{ mol}^{-0.5} \text{ s}^{-1}$ to $3e-10 \text{ m}^{2.5} \text{ mol}^{-0.5} \text{ s}^{-1}$ and $5e-12 \text{ m}^{2.5} \text{ mol}^{-0.5} \text{ s}^{-1}$ to $2.25e-10 \text{ m}^{2.5} \text{ mol}^{-0.5} \text{ s}^{-1}$. The estimated discharge curve and parameter values can be found in Figure 8 and Tables 2.1 and 2.2.

Case Study 4: Estimation of Up, Transport, Kinetic and Design Parameters

In this case study, we estimated Up and all the parameters with wide bounds for SP model at the same time. The bounds for D_p^s and D_n^s were the same as in previous cases. The bounds for k_p and k_n were $3.33e-11 \text{ m}^{2.5} \text{ mol}^{-0.5} \text{ s}^{-1}$ to $1.67e-10 \text{ m}^{2.5} \text{ mol}^{-0.5} \text{ s}^{-1}$ and $2.58e-11 \text{ m}^{2.5} \text{ mol}^{-0.5} \text{ s}^{-1}$ to $1.29e-10 \text{ m}^{2.5} \text{ mol}^{-0.5} \text{ s}^{-1}$. The bounds for R_p and R_n were $2\mu\text{m}$ to $10\mu\text{m}$ and $2.5\mu\text{m}$ to $12.5\mu\text{m}$. While the upper and lower bounds for ε_p and ε_n were 0.3 and 0.6. The results are given in Figure 9 and Tables 2.1 and 2.2.

Error Analysis

The absolute and relevant errors for each case were also calculated, listed in Table 3. The more parameters we estimate at the same time, the greater degree of freedom the solution space has, and thus the smaller error can be achieved compared to the experimental data. Since the parameter values we used in base case were just guesses based on experience, the error incorporated in the parameters, though can be cancelled by varying the parameters we are estimating under this specific condition, may show up under a different operation condition. This is probably what happened in Case 3. Even though the error under 3000mA was smaller compared to Case 1 and 2, the prediction for 600mA, 1000mA and 6000mA was further off. In general, the prediction under lower rates (C/5 and C/3) was better compared to higher rates (2C),

this may result from the limitation of SP model. Since the lithium-ion concentration gradient in the electrolyte is ignored in the SP model, it is only valid under low rates.

Validation

To validate the estimated parameter values got from aforementioned cases, we simulated the discharge behavior at different rates, and compared with experimental data, as shown in Figure 10 (600mA, C/5), 11 (1000mA, C/3), and 12 (6000mA, 2C). As can be observed from the plots, the general discharge performance of the battery under different discharge rates can be predicted reasonably well by our estimated parameters.

Estimation with two discharge curve at different rates might help with the predictability, but using more data means more experiments need to be conducted and more computation need to be run during estimation. Since estimation with one discharge curve can already give us reasonable results under different rate, we will not increase the time and efforts required to get and calculate additional information. However, depending on the application, if higher accuracy is desired, more data points can be easily accommodated in the current optimization framework.

Discussion

All the estimations above were run on a Dell Precision T7500 desktop with two Intel Xeon CPU W5590 3.33GHz processors and 24 GB RAM. We used the Global Optimization Toolbox in MATLAB R2015b in a Windows 7 Professional 64-bit system. The estimation time was under 10 hours for all four cases. Compared with 3 weeks for 88 parameters of P2D model needed for parameter identification on a cluster of five quad-core computers done by Forman et al.⁶ and 19 hours required to identify the parameters of a thermal P2D model on a cluster with 20 cores¹⁴, 10 hours is comparatively good. However, if we want to use the estimation as an on-line monitoring tool, then the computational cost has to be reduced.

In this work, we mainly focused on Up, because the negative electrode of the common commercial cells today is based on graphite, and the OCP of lithium-ion intercalation is well studied, thus readily available when needed. People are pushing the boundary of lithium-ion batteries now, and more material including graphene and silicon is being investigated as potential next-generation battery material. If required, similar to the positive electrode, the linear approximation of negative electrode OCP can be done as well.

Acknowledgement

The authors are grateful for the financial support from the Department of Energy ARPA-E program (Award Number AR0000275) and the Clean Energy Institute at the University of Washington. The authors also want to thank Chintan Pathak for helping them understand the BMS better.

References

1. C. Fleischer, W. Waag, H. Heyn, and D. Sauer, *J. Power Sources* (2014) <http://www.sciencedirect.com/science/article/pii/S0378775314002249>.

2. S. Santhanagopalan, Q. Guo, and R. E. White, *J. Electrochem. Soc.*, **154**, A198 (2007) <http://jes.ecsdl.org/cgi/doi/10.1149/1.2422896>.
3. V. Ramadesigan et al., *J. Electrochem. Soc.*, **158**, A1048 (2011).
4. J. C. Forman, S. J. Moura, J. L. Stein, and H. K. Fathy, *J. Power Sources*, **210**, 263–275 (2012) <http://dx.doi.org/10.1016/j.jpowsour.2012.03.009>.
5. L. Zhang et al., *J. Power Sources*, **270**, 367–378 (2014) <http://dx.doi.org/10.1016/j.jpowsour.2014.07.110>.
6. J. Li et al., *J. Electrochem. Soc.*, **163**, A1646–A1652 (2016) <http://jes.ecsdl.org/lookup/doi/10.1149/2.0861608jes>.
7. M. Doyle, *J. Electrochem. Soc.*, **140**, 1526 (1993).
8. D. Zhang, B. N. Popov, and R. E. White, *J. Electrochem. Soc.*, **147**, 831 (2000).
9. V. Ramadesigan et al., *J. Electrochem. Soc.*, **159**, R31 (2012).
10. Q. Guo and R. White, *J. Electrochem. Soc.* (2005) <http://jes.ecsdl.org/content/152/2/A343.short>.
11. W. Appiah, J. Park, S. Song, S. Byun, and M. Ryou, *J. Power* (2016) <http://www.sciencedirect.com/science/article/pii/S0378775316304037>.
12. P. Ramadass, B. Haran, P. M. Gomadam, R. White, and B. N. Popov, *J. Electrochem. Soc.*, **151**, A196 (2004).
13. S. Lee, J. Kim, J. Lee, and B. Cho, *J. Power Sources* (2008) <http://www.sciencedirect.com/science/article/pii/S0378775308017965>.

Table 1: SPM equations

Governing Equations and Boundary Conditions of Isothermal Model. ($i = p, n$)

	Governing Equations	Boundary Conditions	
Solid phase concentration (cathode): $c_p^s(r, t)$	$\frac{\partial c_p^s}{\partial t} = \frac{1}{r^2} \frac{\partial}{\partial r} \left[r^2 D_p^s \frac{\partial c_p^s}{\partial r} \right]$	$\left. \frac{\partial c_p^s}{\partial r} \right _{r=0} = 0, -D_p^s \left. \frac{\partial c_p^s}{\partial r} \right _{R_p} = \frac{I_{overall}}{A_{cross} l_i a_p F}$	(1.1)
Solid phase concentration (anode) : $c_n^s(r, t)$	$\frac{\partial c_n^s}{\partial t} = \frac{1}{r^2} \frac{\partial}{\partial r} \left[r^2 D_n^s \frac{\partial c_n^s}{\partial r} \right]$	$\left. \frac{\partial c_n^s}{\partial r} \right _{r=0} = 0, -D_n^s \left. \frac{\partial c_n^s}{\partial r} \right _{R_n} = \frac{-I_{overall}}{A_{cross} l_i a_n F}$	(1.2)
Voltage : $V(t)$	$V(t) = \phi_p^s(t) - \phi_n^s(t) - I_{overall} R_c$		(1.3)

Additional equations used in the SPM

Butler-Volmer kinetics:	$\frac{I_{overall}}{A_{cross} l_i a_p F} = k_p \sqrt{c_e c_{p,surf}^s (1 - c_{p,surf}^s)} \sinh \left(\frac{F(\phi_p^s - \phi_{e,p} - U_p)}{2RT} \right)$	(1.4)
	$\frac{-I_{overall}}{A_{cross} l_i a_n F} = k_n \sqrt{c_e c_{n,surf}^s (1 - c_{n,surf}^s)} \sinh \left(\frac{F(\phi_n^s - \phi_{e,n} - U_n)}{2RT} \right)$	(1.5)
Specific Area	$a_i = \left(\frac{3}{R} \right) (1 - \varepsilon_i - \varepsilon_{f,i})$	(1.6)

Table 2.1 Estimated Up Values

SOC	Case1	Case2	Case3	Case4
0.4	4.3464	4.369989257	4.378048843	4.323072203
0.43	4.145	4.140727144	4.312005303	4.117938301
0.46	4.0884	4.096664233	4.261307772	4.065991673
0.49	4.0687	4.066339986	4.211730865	4.052920373
0.52	4.0359	4.022854483	4.161307758	4.01638027
0.55	3.9966	3.985739008	4.111934602	3.957963731
0.58	3.9445	3.942810635	4.062005303	3.931656102
0.61	3.889	3.892814072	4.012152941	3.864245232
0.64	3.8676	3.830109916	3.961786531	3.829605863
0.67	3.7959	3.79085294	3.912423843	3.752775047
0.7	3.7594	3.740805119	3.861314123	3.717424988
0.73	3.6984	3.68161019	3.812174256	3.666763935
0.76	3.6613	3.641084353	3.762710203	3.635575487
0.79	3.6311	3.615505129	3.712897752	3.595143106
0.82	3.5805	3.563430737	3.663692959	3.538127463
0.85	3.5373	3.514910551	3.610132329	3.496631836
0.88	3.4841	3.461853964	3.560271627	3.434113624
0.91	3.4139	3.390614046	3.509807948	3.351897228
0.94	3.3173	3.285709317	3.407893519	3.230883049
0.97	3.1506	3.068522404	3.239287855	2.968435316
0.99	2.7847	2.641094113	2.857889393	2.625952316

Table 2.2 Estimated Parameters with Up

		Unit	Case 2	Case 3	Case 4	Base Case	Reported in Ref. 11
Transport Parameters	D_p^s	$\text{m}^2 \text{s}^{-1}$	6.7108e-13	3.4832e-13	3.4848e-13	6.6756e-13	9.98e-13
	D_n^s	$\text{m}^2 \text{s}^{-1}$	2.6174e-12	1.0211e-12	1.0618e-12	2.0085e-12	1.57e-14
Kinetic Parameters	k_p	$\text{m}^{2.5} \text{mol}^{-0.5} \text{s}^{-1}$	-	3.4710e-11	3.5898e-11	1.334e-10	3.94e-11
	k_n	$\text{m}^{2.5} \text{mol}^{-0.5} \text{s}^{-1}$	-	1.0046e-10	7.9500e-11	1.0307e-10	3e-11
Design Parameters	R_p	μm	-	-	2.63	8	4.5
	R_n	μm	-	-	2.0	10	10.5
	l_p	μm	-	-	42.59	43	30
	l_n	μm	-	-	46.04	46.5	54
	ε_p	-	-	-	0.421	0.423	0.2
	ε_n	-	-	-	0.409	0.413	0.37

Table 3 Error Analysis for various case studies

Case Study	Absolute Error	Relative Error
Up + R	0.0031	2.9886e-04
Up + Transport	0.0033	3.1239e-04
Up + Transport + Kinetic	4.5170e-04	3.4846e-05
Up + Transport + Kinetic + Design	2.3177e-04	2.0359e-05

$$\text{Absolute Error} = \frac{|V - V_{\text{expt}}|}{n} \quad (5)$$

$$\text{Relative Error} = \frac{|V - V_{\text{expt}}|}{nV_{\text{expt}}} \quad (6)$$

Figures

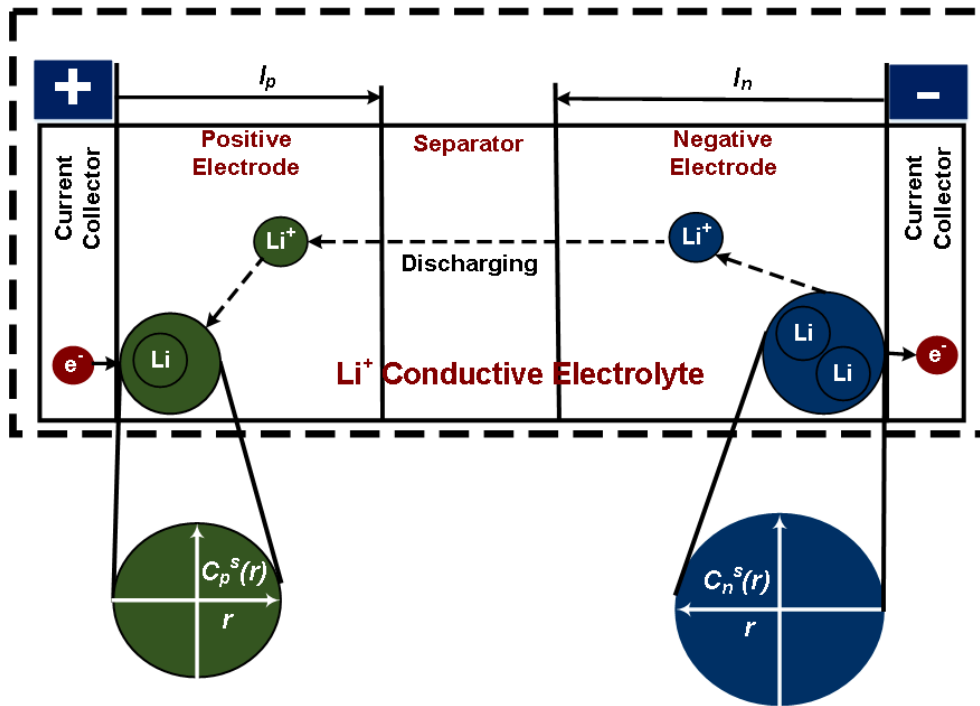


Figure 1 Schematic of the Single Particle Model

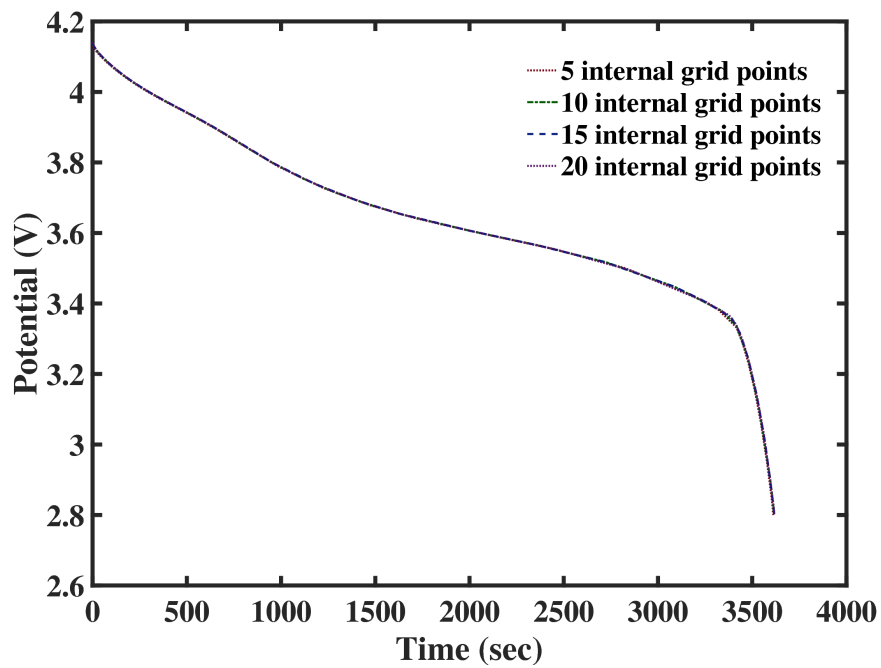


Figure 2 Selection of number of node points for finite difference method

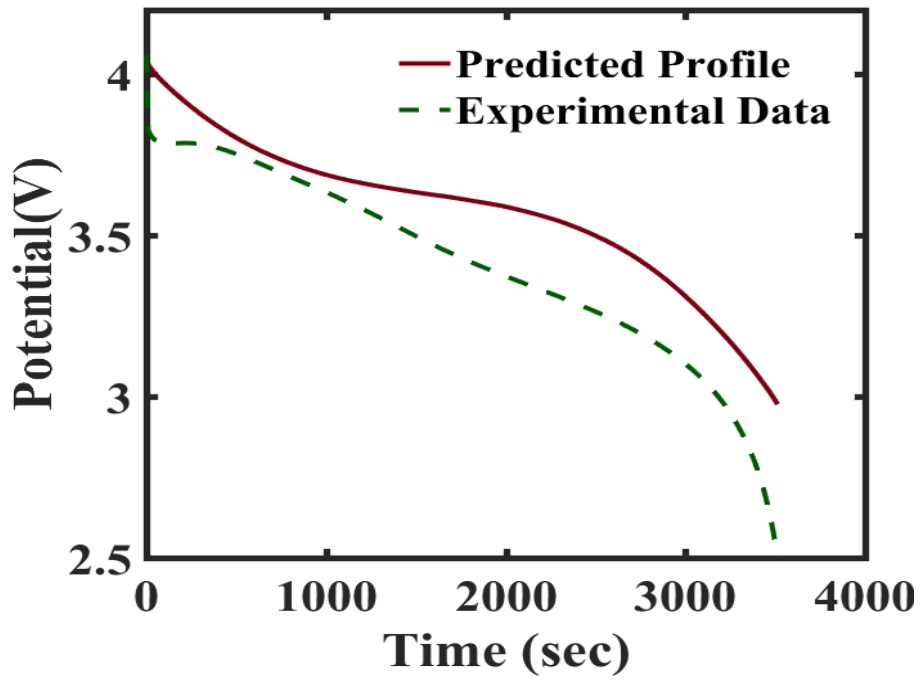


Figure 3 Estimation of U_p using polynomial function

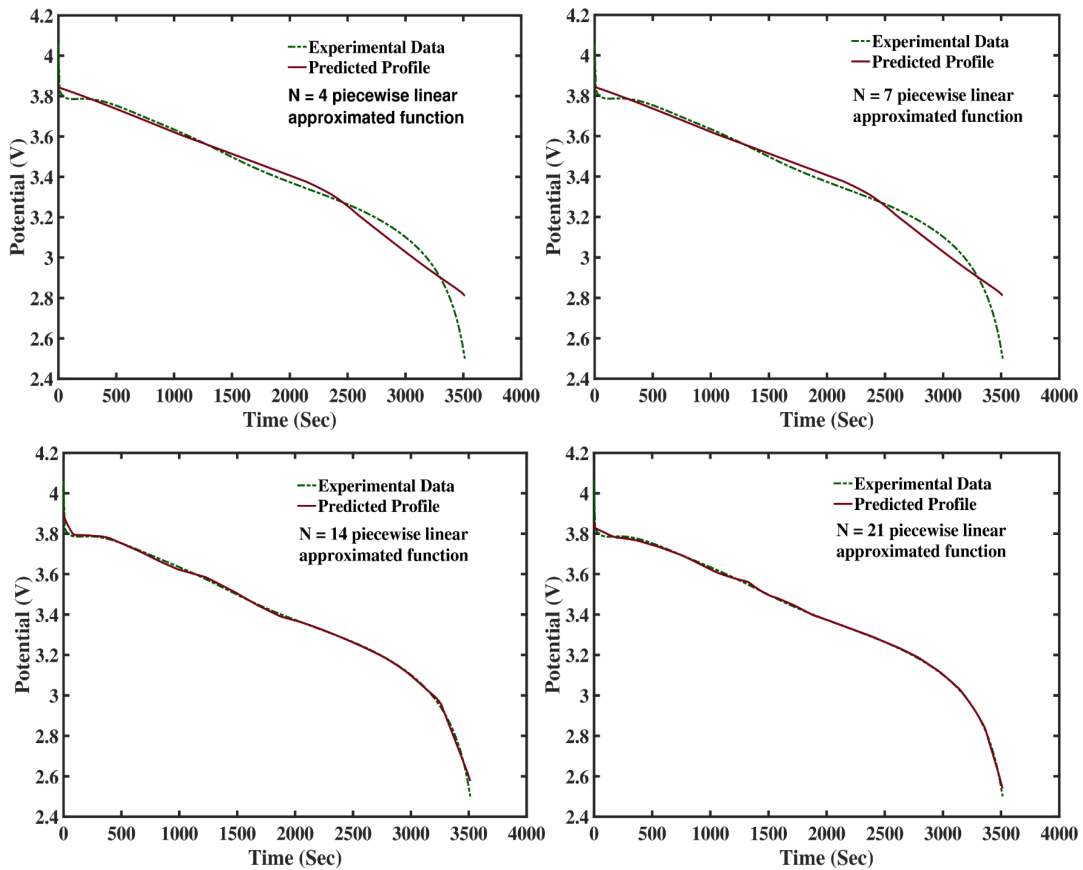


Figure 4 Selection of number of piecewise linear approximation functions

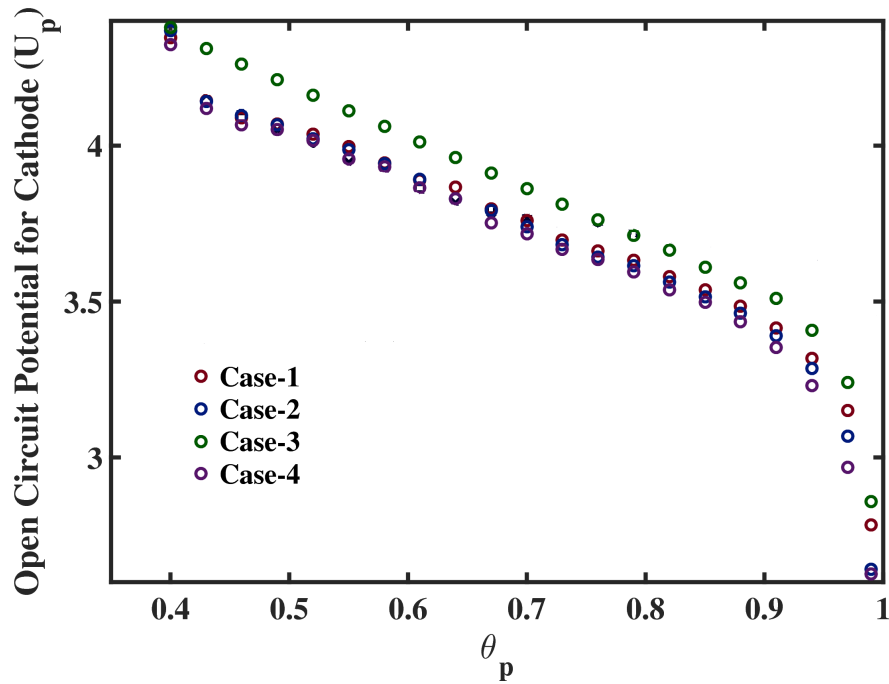


Figure 5 Predicted profile of open circuit potential of the positive electrode using piecewise linear approximation function for each cases

Case – 1: Estimation of open circuit potential of cathode using piece wise linear approximation function along with Resistance.

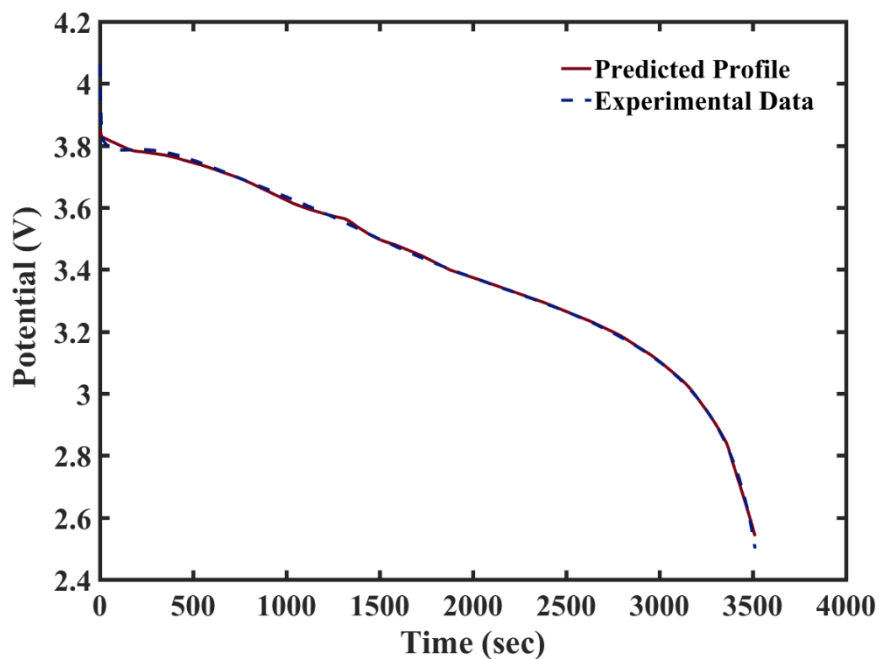


Figure 6 Potential profile using predicted values of open circuit potential of cathode

Case – 2: Estimation of open circuit potential of cathode using piece wise linear approximation function along transport parameters

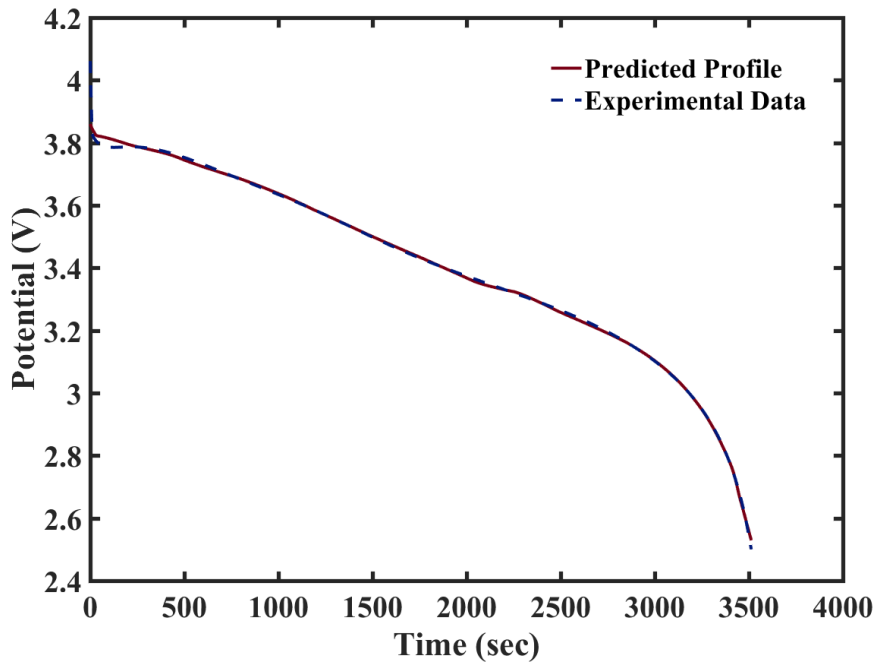


Figure 7 Potential profile using predicted values of open circuit potential of cathode and transport parameters

Case – 3: Estimation of open circuit potential of cathode using piece wise linear approximation function along with transport parameters and kinetic parameters

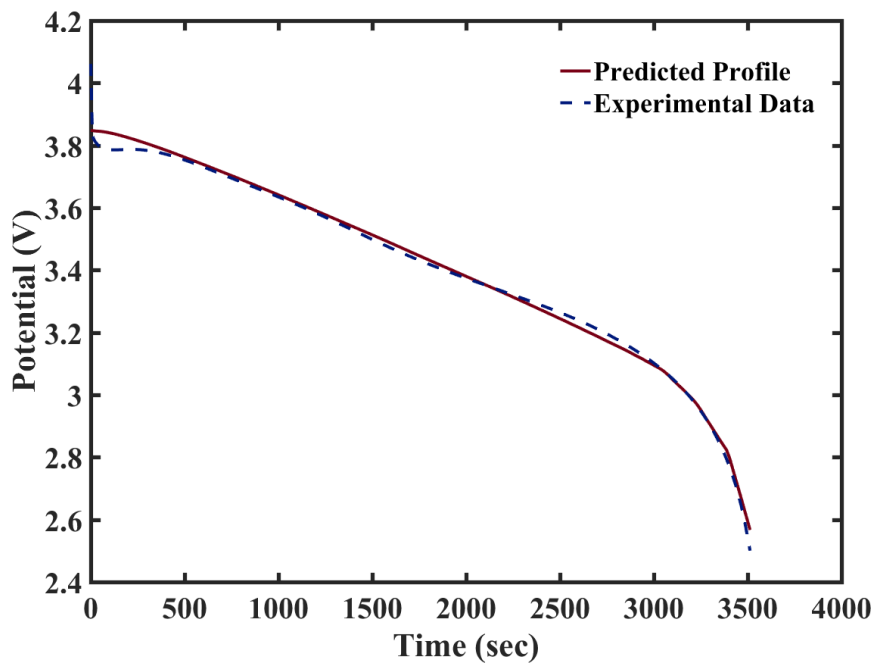


Figure 8 Potential profile using predicted values of open circuit potential of cathode, transport and kinetic parameters

Case – 4: Estimation of open circuit potential of cathode using piece wise linear approximation function along with transport, kinetic parameters and design parameters

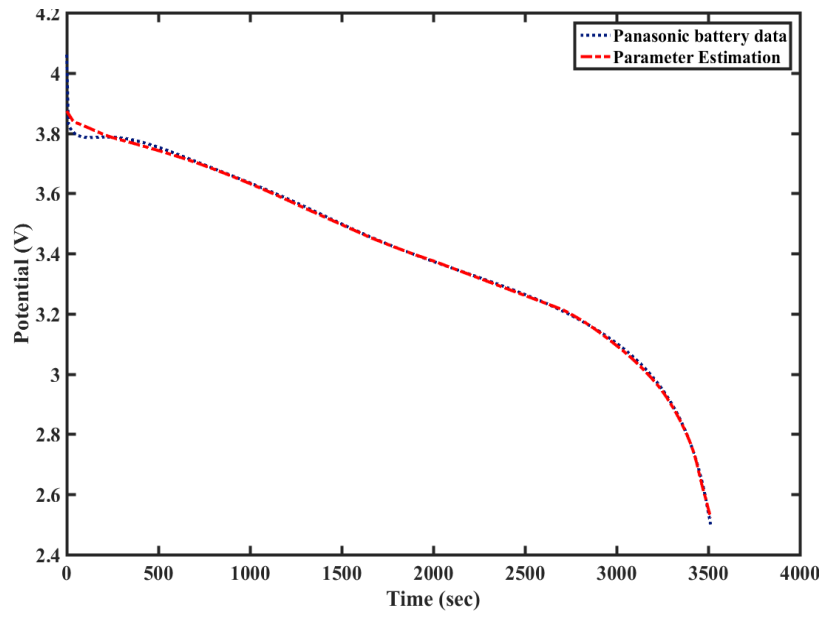


Figure 9 Potential profile using predicted values of open circuit potential of cathode along with transport, kinetic and design parameters

Validation

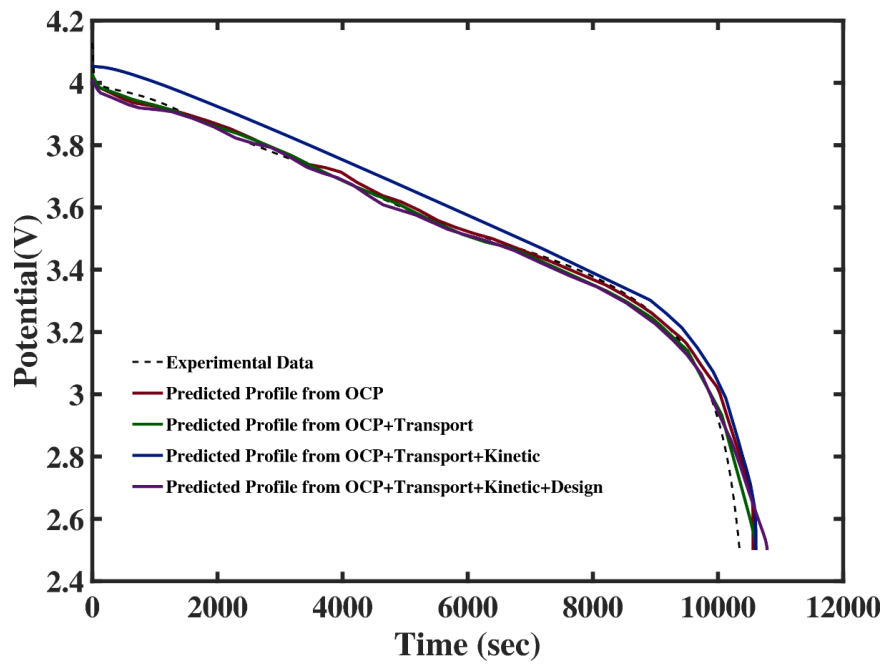


Figure 10 Comparisons of different parameter estimation case studies with the experimental data for 1000mA

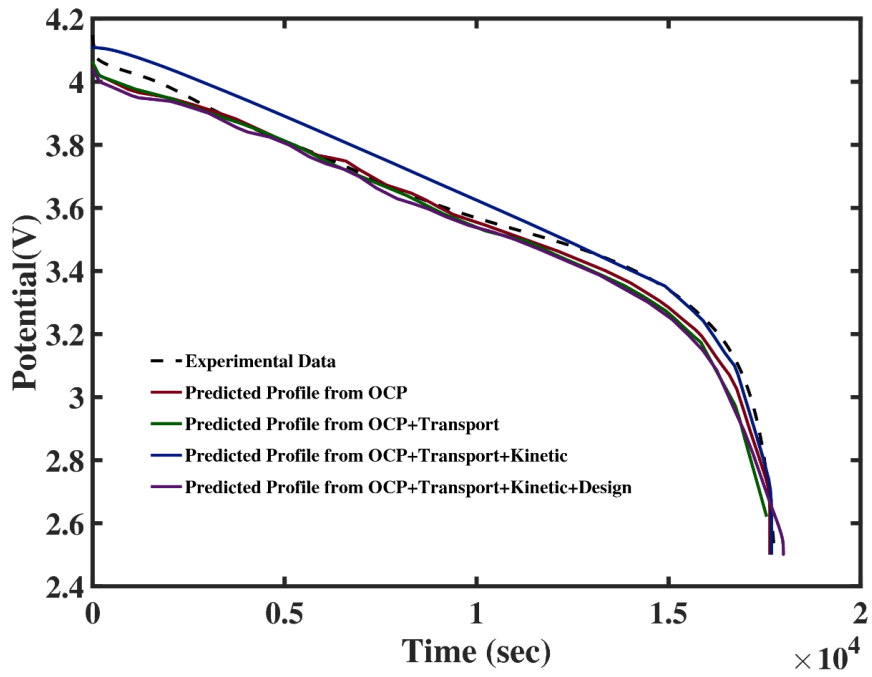


Figure 11 Comparisons of different parameter estimation case studies with the experimental data for 600mA

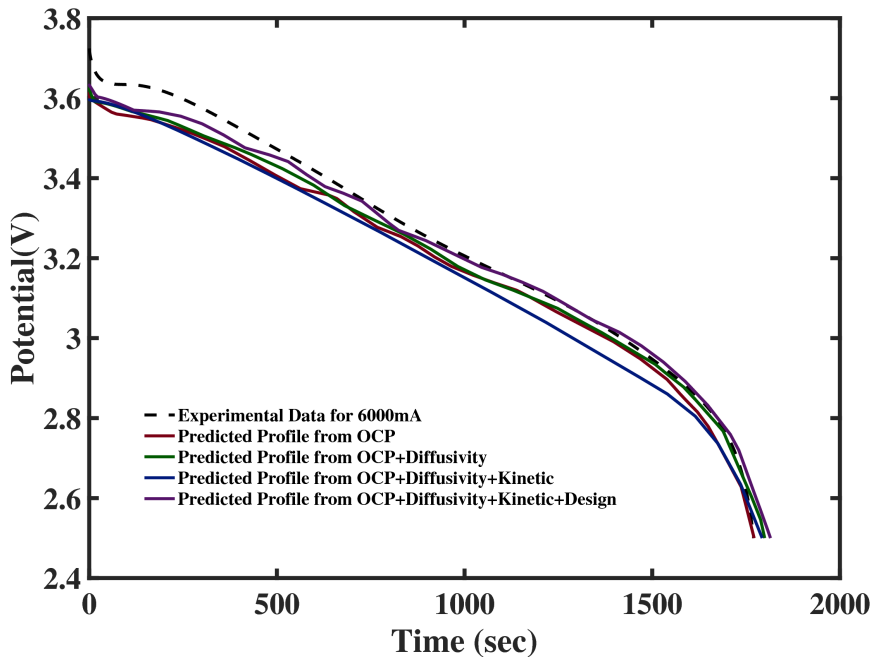


Figure 12 Comparisons of different parameter estimation case studies with the experimental data for 6000mA